



Gas-phase reactions of halogenated radical carbene anions with sulfur and oxygen containing species

Stephanie M. Villano, Nicole Eyt, W. Carl Lineberger, Veronica M. Bierbaum*

JILA, University of Colorado and the National Institute of Standards and Technology and Department of Chemistry and Biochemistry, University of Colorado, Boulder, Colorado 80309-0440, United States

ARTICLE INFO

Article history:

Received 4 April 2008

Received in revised form 1 July 2008

Accepted 15 July 2008

Available online 25 July 2008

Keywords:

Selected-ion flow tube

Carbene anion

Radical anion

Nucleophilic displacement

Ion–molecule reaction

ABSTRACT

The reactivities of mono- and dihalocarbene anions ($\text{CHCl}^{\bullet-}$, $\text{CHBr}^{\bullet-}$, $\text{CF}_2^{\bullet-}$, $\text{CCl}_2^{\bullet-}$, and $\text{CBrCl}^{\bullet-}$) were studied using a tandem flowing afterglow-selected ion flow tube instrument. Reaction rate constants and product branching ratios are reported for the reactions of these carbene anions with six neutral reagents (CS_2 , COS , CO_2 , O_2 , CO , and N_2O). These anions were found to demonstrate diverse chemistry as illustrated by formation of multiple product ions and by the observed reaction trends. The reactions of $\text{CHCl}^{\bullet-}$ and $\text{CHBr}^{\bullet-}$ occur with similar efficiencies and reactivity patterns. Substitution of a Cl atom for an H atom to form $\text{CCl}_2^{\bullet-}$ and $\text{CBrCl}^{\bullet-}$ decreases the rate constants; these two anions react with similar efficiencies and reactivity trends. The $\text{CF}_2^{\bullet-}$ anion displays remarkably different reactivity; these differences are discussed in terms of its lower electron binding energy and the effect of the electronegative fluorine substituents. The results presented here are compared to the reactivity of the $\text{CH}_2^{\bullet-}$ anion, which has previously been reported.

© 2008 Elsevier B.V. All rights reserved.

1. Introduction

Simple halogen substituted carbenes (CXY , where $\text{X} = \text{F}$, Cl , and Br and $\text{Y} = \text{H}$, F , Cl , and Br) have singlet ground states [1–3]. In solution, these molecules are highly reactive and undergo characteristic reactions such as insertion into single bonds and cycloaddition to double bonds [4,5], making them useful synthetic organic chemistry reagents. In the atmosphere, these compounds are likely photofragments of chlorofluoro compounds and other halons [6–10]; the role of halogenated compounds in ozone depletion has been well documented [11–14]. In addition, the reactions of halocarbenes are important to the plasma chemistry of halogenated compounds [15] and to organometallic chemistry [16–18].

There has been an extensive effort, both experimentally and theoretically, aimed at determining the fundamental physical properties of halocarbenes. These studies have been employed to determine the electronic and molecular structure of the ground and first excited state, vibrational frequencies, ionization energies, electron affinities, and the singlet–triplet splittings [1–3,19–46]. Additionally, heats of formation, gas-phase acidities, and bond dissociation energies have been determined either directly or indi-

rectly through gas-phase ion–molecule bracketing experiments and collision-induced dissociation threshold energy measurements [47–52].

While halogen substituted neutral carbenes have been extensively investigated, only a few studies have addressed the chemistry of the corresponding anions. Addition of an electron to a halocarbene forms a π -radical anion [1–3]. In solution, radical anions are of interest since these species are often reactive intermediates. In the gas-phase, the chemistry of radical anions has important implications for reactions in the upper atmosphere [53], negative ion chemical ionization mass spectrometry [54,55], and electron capture detectors [56].

The majority of the studies involving $\text{CXY}^{\bullet-}$ anions have focused on electron and proton transfer reactions [50–52]; these studies have provided valuable thermodynamic information about the corresponding neutral carbenes. Beyond this, Born et al. [50,57] have investigated the reactivity of a series of monohalocarbene anions with methyl halides, organic esters, and aliphatic alcohols. Their results show that reactions with methyl halides proceed solely by an $\text{S}_{\text{N}}2$ mechanism, while the reactions with the esters proceed by competing $\text{S}_{\text{N}}2$ and $\text{B}_{\text{AC}}2$ mechanisms [57]. The reactions with the alcohol series (ROH) indicate that, in addition to proton transfer, an $\text{S}_{\text{N}}2$ reaction to produce X^- also occurs. This $\text{S}_{\text{N}}2$ process must occur within the $[\text{RO}^- + \text{CH}_2\text{X}]$ complex before the initial products separate [50]. Recently, we investigated the reactions of $\text{CHCl}^{\bullet-}$ with a series of chloromethanes [58]. These reactions primarily occur via substitution and proton transfer. Additionally, however,

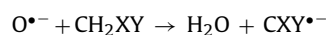
* Corresponding author. Tel.: +1 303 492 7081; fax: +1 303 492 5894.
E-mail address: veronica.bierbaum@colorado.edu (V.M. Bierbaum).

isotopic labeling studies indicate that carbene anions can undergo an insertion–elimination mechanism, where the anion inserts into a C–Cl bond to form an unstable intermediate, which eliminates either $\text{Cl}_2^{\bullet-}$ or Cl^- and Cl^\bullet .

In this study we evaluate the gas-phase reactivity of simple substituted carbene anions with a series of oxygen and sulfur containing neutral reagents (CS_2 , COS , CO_2 , O_2 , CO , and N_2O). In past studies from our laboratory, we have found that this series of neutral reagents can provide insight into the structure of an anion as well as form interesting product ions from diverse chemistry [59–67]. Additionally, the reactivity of methylene anion, $\text{CH}_2^{\bullet-}$, has been studied with this neutral series [65], which allows for direct comparison to the results presented here. In this work we have measured reaction rate constants as well as product ion branching ratios. Additionally, we suggest reaction mechanisms, which account for the observed product ions. Since there is very little thermochemical information available in the literature for these systems, electronic structure calculations are employed to evaluate the reaction exothermicities for several proposed pathways.

2. Experimental

The reactivities of mono- and dihalocarbene anions ($\text{CHCl}^{\bullet-}$, $\text{CHBr}^{\bullet-}$, $\text{CF}_2^{\bullet-}$, $\text{CCl}_2^{\bullet-}$, and $\text{CBrCl}^{\bullet-}$) were studied using a tandem flowing afterglow-selected ion flow tube instrument (FA-SIFT), which has previously been described [68]. Reactant ions were formed in a flowing afterglow source from the $\text{H}_2^{\bullet+}$ abstraction reactions of $\text{O}^{\bullet-}$ [69,70]:



Ions of a single isotopomer were mass-selected and injected into a reaction flow tube where they were thermalized to 302 ± 2 K by collisions with He buffer gas (0.5 torr, $\sim 10^4$ cm s⁻¹). Despite injecting the reactant ions with minimal energy, X^- ions produced from collision-induced dissociation were also present in the reaction flow tube; the presence of these additional ions was considered in the data analysis below.

Measured flows of neutral reagents were introduced into the reaction flow tube through a manifold of inlets and the reactant and product ions were analyzed by a quadrupole mass filter coupled to an electron multiplier. Reaction rate constants were determined by changing the neutral reagent inlet position, thereby varying the reaction distance and time, while monitoring the change in reactant ion intensity. Product branching fractions were measured at each neutral inlet and averaged together; secondary reactions in general do not occur for these systems. Efforts were made to minimize mass discrimination, however, it was necessary to estimate the relative detection sensitivities when calculating product branching ratios. The relative detection sensitivity was estimated by examining a series of exothermic ion–molecule reactions where only one ionic product was formed. For reactions of $\text{CBrCl}^{\bullet-}$, we were unable to cleanly separate the $\text{CBrCl}^{\bullet-}$ anion from the CHBrCl^- anion in the

injection process. The presence of this additional ion does not interfere with measurements of the overall reaction rate constant since $\text{CBrCl}^{\bullet-}$ can be resolved and monitored with the mass detection system. The presence of CHBrCl^- , however, does complicate the determination of the product branching ratios. For this same reason, the $\text{CBr}_2^{\bullet-}$ anion was not included in this study. Additionally the $\text{CHF}^{\bullet-}$ anion was not studied since it occurs at the same mass as $\text{O}_2^{\bullet-}$, which is also present in the ion source.

The error reported for the reaction rate constants is one standard deviation of at least three measurements. The uncertainty in the reaction rate constants due to systematic error is $\pm 20\%$ and the uncertainty in the product branching ratios is $\pm 30\%$. Helium buffer gas (99.995%) was purified by passage through a liquid nitrogen-cooled molecular sieve trap. Neutral reagents were purchased from commercial sources and used without further purification. The reactions of $\text{CXY}^{\bullet-}$ with COS indicate that the neutral sample contains a trace amount of H_2S impurity; as a result, the measured rate constants represent an upper bound value. The reported reaction efficiencies are the measured rate constant divided by the calculated collision rate constant ($\text{eff} = k/k_{\text{col}}$). Collision rate constants were calculated from parameterized trajectory collision rate theory [71].

Electronic structure calculations were performed using the G3 composite technique [72] provided in the Gaussian 03 suite of programs [73]. The electronic energy, harmonic frequencies, and rotational constants were determined for the optimized geometries of the reactants and products of the fluorinated and chlorinated reactions. These results were used to evaluate the exothermicities of the proposed mechanisms; a more detailed investigation to include the reaction intermediates and transition states is beyond the scope of this work. The exothermicities of the brominated reactions are not provided since the G3 method does not include fourth row elements. The Cartesian coordinates and energies for the optimized geometries of the reactants and products are provided in the [Supplementary Information](#).

3. Results and discussion

Table 1 displays the experimentally measured reaction rate constants for the reactions of $\text{CXY}^{\bullet-}$ with each neutral reagent; Table 2 presents product ion branching fractions. Fig. 1 is a plot of reaction efficiency as a function of anion basicity for the reactions of $\text{CXY}^{\bullet-}$ with CS_2 , COS , CO_2 , O_2 , and CO ; N_2O is excluded from this plot since it only reacts with $\text{CF}_2^{\bullet-}$. In this figure each trace represents a different neutral reagent and the data points are connected to guide the eye only. The reaction trends presented in this plot are not readily observed in Table 1 since the collision rate constants for the reactions of CO_2 and CS_2 are smaller than for COS . The $\text{CHCl}^{\bullet-}$ and $\text{CHBr}^{\bullet-}$ anions react with similar efficiencies and trends. As expected, replacing a hydrogen atom with a chlorine atom to form $\text{CCl}_2^{\bullet-}$ and $\text{CBrCl}^{\bullet-}$ substantially decreases the reaction efficiency. The reaction efficiencies and trends for the $\text{CCl}_2^{\bullet-}$ and $\text{CBrCl}^{\bullet-}$

Table 1
Reaction rate constants (10^{-10} cm³ s⁻¹) for the reactions of $\text{CXY}^{\bullet-}$ with CS_2 , COS , CO_2 , O_2 , CO , and N_2O

Neutral reagent	$\text{CHCl}^{\bullet-}$ (384.8; 1.210) ^a	$\text{CHBr}^{\bullet-}$ (380.7; 1.454)	$\text{CF}_2^{\bullet-}$ (377.4; 0.180)	$\text{CCl}_2^{\bullet-}$ (364.2; 1.590)	$\text{CBrCl}^{\bullet-}$ (361; 1.84)
CS_2	10.5 ± 0.7^b	9.14 ± 0.22	10.7 ± 0.3	0.400 ± 0.080	0.162 ± 0.009
COS^c	6.87 ± 0.25	5.27 ± 0.14	5.02 ± 0.17	1.31 ± 0.03	0.850 ± 0.038
CO_2	5.62 ± 0.17	5.13 ± 0.02	$<0.070 \pm 0.002$	<0.001	<0.001
O_2	2.11 ± 0.04	1.80 ± 0.05	2.65 ± 0.03	0.946 ± 0.025	0.748 ± 0.014
CO	1.42 ± 0.25	0.943 ± 0.013	<0.001	<0.001	<0.001
N_2O	<0.001	<0.001	0.178 ± 0.030	<0.001	<0.001

^a The enthalpy of protonation in kcal mol⁻¹ and the electron binding energy in eV are given in parentheses; see Refs. [2,3,50,51].

^b Standard deviation of at least three measurements.

^c Reaction rate constants represent an upper bound value, see experimental section.

Download English Version:

<https://daneshyari.com/en/article/1194799>

Download Persian Version:

<https://daneshyari.com/article/1194799>

[Daneshyari.com](https://daneshyari.com)